Embedded Model Control calls for disturbance modeling and rejection

(Article begins on next page)

20 May 2024

Embedded Model Control calls for disturbance modeling and rejection

Enrico Canuto, Wilber Acuna-Bravo, Andrés Molano-Jimenez, Carlos Perez Montenegro

Politecnico di Torino, Dipartimento di Automatica e Informatica

Corso Duca degli Abruzzi 24, 10129 Torino, Italy

enrico.canuto@polito.it

ABSTRACT

Robust control design is mainly devoted to guaranteeing the closed-loop stability of a model-based control law in the presence of parametric uncertainties. The control law is usually a static feedback law which is derived from a (nonlinear) model using different methodologies. From this standpoint, stability can only be guaranteed by introducing some ignorance coefficients and restricting the feedback control effort with respect to the model-based design. Embedded Model Control shows that, the model-based control law must and can be kept intact in the case of uncertainty, if, under certain conditions, the controllable dynamics is complemented by suitable disturbance dynamics capable of real-time encoding the different uncertainties affecting the 'embedded model', i.e. the model which is both the design source and the core of the control unit. To be real-time updated the disturbance state is driven by an unpredictable input vector, the noise, which can only be estimated from the model error. The uncertainty-based (or plant-based) design concerns the noise estimator, so as to prevent the model error from conveying uncertainty components (parametric, cross-coupling, neglected dynamics) which are command-dependent and thus prone to destabilizing the controlled plant, into the embedded model. Separation of the components in the low and high frequency domain by the noise estimator itself allows stability recovery and guarantee, and the rejection of low frequency uncertainty components. Two simple case studies endowed with simulated and experimental runs will help to understand the key assets of the methodology.

KEYWORDS：Embedded Model Control, disturbance, noise estimator, rejection, model error

No.	Symbol	Explanation	Equation	Comments
Table 1. List of variables				
0	$\mathbf{d}$	Input disturbance	(2), (8)	
1	$\mathbf{d}_u, \hat{\mathbf{d}}_u$	Collocated disturbance, predicted	(9), (30)	
2	$\mathbf{d}_y$	Output disturbance	(39)	
3	$\partial \mathbf{P}$	Fractional error dynamics	(17)	Uncertain
4	$\mathbf{e}$	Model error (output)	(1)	
5	$\overline{\mathbf{e}}$	'Estimated' model error (output)	(25)	
6	$\hat{\mathbf{e}}_c$	Prediction error	(24)	
7	$\underline{\mathbf{e}}_y$	'True' tracking error (output)	(23)	$\underline{\mathbf{e}}_y = C_c \underline{\mathbf{e}}$
8	$\underline{\mathbf{e}}$	'True' tracking error (state)	(23)	
9	$\hat{\underline{\mathbf{e}}}$	'Estimated' tracking error (state)	(24)	
10	$\hat{\underline{\mathbf{e}}}_y$	'Estimated' tracking error (output)	(24)	
11	$\mathbf{e}_y$	Control error (jitter)	(26)	$\mathbf{e}_y = \hat{\underline{\mathbf{e}}}_y - \overline{\mathbf{e}}$
12	$\mathbf{h}$	Cross-coupling (parametric uncertainty)	(8)	Uncertain
13	i, f	Discrete-time instant, frequency		from $t_i = iT$
14	λ, γ	Discrete-time eigenvalue, complementary eigenvalue		$\gamma = 1 - \lambda$
15	$\mathbf{m}, \underline{\mathbf{m}}$	Collocated cross-coupling, known	(9), (33)	
16	$\varDelta \mathbf{m}$	Cross-coupling error	(33)	Uncertain
17	$\mathbf{M}$	Controllable dynamics	(18)	Input-output
18	$\mathbf{P}$	Design model dynamics	(18)	Uncertain
19	$\mathbf{q}$	State vector of a dynamic noise estimator	(12)	
20	$\mathbf{S}_m, \mathbf{V}_m$	Predictor sensitivity, sensitivity complement	(40)	
21	$\mathbf{u}$	Discrete-time real-valued command	(2)	Digitized as $\tilde{\mathbf{u}}$
22	$\underline{u}$	Reference command	(5)	univariate
23	$T, f_{\max}$	Model and control time unit, Nyquist frequency		
24	$\mathbf{x}_c, \hat{\mathbf{x}}_c$	Controllable state, predicted state	(2), (24)	
25	$\underline{\mathbf{x}}$	Reference state	(5)	
26	$\mathbf{x}_d, \hat{\mathbf{x}}_d$	Disturbance state, predicted state	(8), (30)	
27	$\mathbf{x}_y$	Output disturbance state	(39)	
28	$\mathbf{w}$	(White) noise vector	(8)	
29	$\mathbf{w}_u, \overline{\mathbf{w}}_u$	Collocated noise, estimated noise	(9), (29)	
30	$\mathbf{w}_y$	Measurement noise	(17)	
31	$\mathbf{y}$	Discrete-time real-valued measure	(1)	Digitized as $\tilde{\mathbf{y}}$

32	$\mathbf{y}_m$	Model output	(1)	
33	$\underline{\mathbf{y}}$	Reference output	(5)	

1 INTRODUCTION

1.1 *The goal and rationale of the paper*

Robust control design [1] is devoted to guaranteeing the closed-loop stability of a model-based control law in the presence of parametric uncertainties. The law is usually a complex feedback algorithm which is derived from a (nonlinear) model using different methodologies. Stability is guaranteed by introducing some ignorance coefficients and restricting the feedback control effort with respect to the model-based design. Embedded Model Control (EMC) [2] shows that a model-based control law must and can be kept intact in the case of uncertainty (a form of separation theorem), if the controllable dynamics is complemented with suitable disturbance dynamics capable of real-time encoding the different uncertainties affecting the 'embedded model', i.e. the model which is both the design source and the core of the control unit. The disturbance state is updated in real-time by an unpredictable input vector, referred to as noise, which can be estimated from the model error only, the latter being defined as the difference between plant and model output. The uncertainty (or plant)-based design concerns the noise estimator, as the model error may convey uncertainty components (parameters, cross-couplings, neglected dynamics) which are command-dependent and thus are prone to destabilize the controlled plant, into the embedded model. Appropriate separation of the uncertainty components into low and high frequency domains by the noise estimator allows stability recovery and guarantee, and the rejection of the low frequency uncertainty components. Emphasis will be given to a single control unit. Two case studies will help to understand the key assets of the methodology.

1.2 *Paper organization*

A goal of Embedded Model Control is to offer a way of converting model and control architecture into real-time code, taking for granted that model and control architecture should

not be completely free, but constrained and guided by some basic principles (axioms and propositions), such as, for instance, that the sole feedback channel is noise, or the core of a control unit is the embedded model. The surprising point is that, when searching for literature with keywords like 'control' and 'axioms/propositions' only software engineering papers can be found [3], [4], [5], which have no or little relation to the immense bulk of control literature, as if control theory and implementation could run separate, leaving the latter to electrical and software engineering tools. In an effort to fill the gap, the paper is organized into a sequence of propositions, aiming at fixing the basic and compulsory principles of model and control architecture, design and implementation. This is done with the help of the system and control theory at the foundations of the EMC, and with reference to control textbooks and papers.

Propositions, that are provable, are subdivided into two parts: model and control. Model propositions start from plant and model distinction, leading to the definition of the model error, that is the key measurable variable of control design and performance (Section 2.2). To reduce unavoidable drifts of the model error, controllable dynamics must be enriched with disturbance dynamics driven by noise (Section 2.3). As a key result, noise (and noise estimator) constitutes the sole feedback channel - to be designed - from plant to model (Section 2.4). The resulting embedded model is further enriched (design model) by the class of the command dependent discrepancies (parametric uncertainties, neglected dynamics) that are zeroed in the control unit, but are essential for robust design and assessment (Section 2.5). The design model is implemented in the form of a numerical simulator, and as such may surrogate the plant during design assessment. A logical consequence of the model propositions is that the noise estimator design is a modeling stage, unlike [2], which must guarantee that the model error becomes bounded whatever the actuating commands may be. A bounded model error implies that model and plant are tracking each other within some frequency domain, a prerequisite to the model-based design as confirmed by the control propositions in Section 3.1.

Control propositions start with the definition of the tracking error as a performance variable, and show that the standard control error (reference minus measurements) is the sum of

tracking and model errors (Section 3.1). Since the former is model-based, the central theorem of the paper shows it can be brought to zero in the 'anti-causal' limit, and the latter can be approached 'in practice' by pushing the model-based feedback to be deadbeat (unless actuator limits exist), without considering model discrepancies (model-based design, Section 3.2). Uncertainties are accommodated by the noise estimator, or, better, by the state predictor, which, in the anti-causal limit, becomes entirely responsible for plant stability (Section 3.3). The corresponding uncertainty-based design is only outlined, but is somewhat detailed in the case study section.

Part of the principles and results expressed in the paper propositions derive from a reorganization of [2], aiming at a logical and complete sequence of design and implementation principles. Many details of [2] are omitted. Advances and simplifications are as follows.

1) The uncertainty propositions in Section 2.3 and the relevant state equations (8) include the nonlinear term $\mathbf{h}(\cdot)$ accounting for parametric uncertainty. A distinction is made between the embedded model, which being free of unmodelled uncertainty is coded in the control unit, and the design model including all the uncertainty components.

2) Performance propositions in Section 3.1 prove and suggest the need for a model and uncertainty-based design decomposition.

3) Theorem 1 in Section 3.2.1 details the necessary and sufficient conditions for the model-based tracking errors being bounded in the presence of unknown nonlinear terms $\mathbf{h}(\cdot)$. The key condition, besides internal stability, is that the estimated noise forcing the tracking error is bounded. The unrealizable 'anti-causal limit', that has been already defined in [2], is repeated and discussed as a model-based concept. Under this limit the tracking error equation becomes autonomous.

4) The uncertainty-based design, briefly dealt with in Section 3.3, demonstrates the trade-off between two contrasting objectives: (i) blocking the response of the neglected dynamics from entering the estimated noise, (ii) enlarging the bandwidth of the parametric uncertainty response entering the estimated noise.

Two case studies are presented. The first case, only simulated, considers a single degree-of-freedom spacecraft [6], [7], whose attitude is measured by a sensor on a flexible appendage. If the position control design assumes a single rigid body from command to sensor, it must be guaranteed against the neglected dynamics from body to sensor. The second case, both simulated and experimental, considers a ball and beam device [8], where the beam is driven by a dc motor through a gear affected by backlash. The ball moves along the beam but is not controlled. A control design similar to the former case is applied, except for a simpler disturbance model. Again the design assumes a rigid body from motor to beam, thus neglecting gear dynamics.

2   Model propositions

2.1   Time, signals and the extended plant

Continuous time is denoted by t. Discrete-time (DT) instants are denoted by $t_i = iT$, assuming T is the least and constant time unit. Real-valued DT signals are indicated by $\mathbf{u}(i)$. They are different from 'digital signals' $\tilde{\mathbf{u}}(i)$, defined as integer-valued and bounded. Computer-based control receives from and dispatch to plant only measures $\tilde{\mathbf{y}}(i)$ and commands $\tilde{\mathbf{u}}(i)$. $\tilde{\mathbf{y}}(i)$ is the sampled and digitized signal (ADC) of the sensor analogue output. $\tilde{\mathbf{u}}(i)$ is converted by a DAC into a step-wise analogue voltage driving the plant. To avoid dealing with integer values, $\tilde{\mathbf{u}}$ is digitized from a real-valued command $\mathbf{u}(i)$ (A/D conversion), whereas $\tilde{\mathbf{y}}(i)$ is converted to a real-valued measure $\mathbf{y}(i)$ (D/A conversion). Conversions take place in the control unit and should not be confused with conversions made by DAC and ADC. The 'extended plant' to be modeled and controlled is defined as the whole chain from $\mathbf{u}(i)$ to $\mathbf{y}(i)$. Thus a DT equation fits.

2.2   The fundamental input-output propositions

2.2.1   Propositions

Modern control design is a chapter of the dynamical system theory [9], which includes concepts and methods like controllability, observability and feedback regulation [10].

'Propositions' should first lead to an appropriate model of the extended plant. Distinguishing between plant (reality) and (mathematical) model $\mathbf{M}$ leads to two propositions.

1) *Proposition 1.* A model can run in parallel and synchronous (in real-time) with the plant under the same command $\mathbf{u}$. The statement is seminal to all the subsequent formulation, and to control architecture as well, as it suggests that control units should be developed around the real-time model, henceforth indicated as the 'embedded model'. When restricted to a computer-based control, a real-time model can only be DT and state-variable [10], implying that a time unit T and a state $\mathbf{x}_c$ must be defined.

2) *Proposition 2.* This concerns model performance, asserting that plant and model, running in parallel, can be compared only through the model error $\mathbf{e}$, which is the difference between the plant output $\mathbf{y}$ (measures) and the model output $\mathbf{y}_m$ as follows

$$\mathbf{e}(i) = \mathbf{y}(i) - \mathbf{y}_m(i). \tag{1}$$

Performance as a suitable norm $|\mathbf{e}|$ may be unbounded, because of unmeasurable, indescribable and uncertain discrepancies between reality (plant) and mathematics (model). Discrepancies may be due to command–independent actions (disturbance), parametric uncertainty, neglected interactions and dynamics. The substantive attribute 'uncertainty' will substitute 'discrepancy' throughout.

2.2.2   The controllable dynamics

Assuming strict causality, linearity, time–invariance and a single time unit, the state equations of $\mathbf{M}$ are written as

$$\begin{aligned} \mathbf{x}_c(i+1) &= A_c\mathbf{x}_c(i) + B_c\mathbf{u}(i) + \mathbf{d}(i), \ \mathbf{x}_c(0) = \mathbf{x}_{c0} \\ \mathbf{y}(i) &= C_c\mathbf{x}_c(i) + \mathbf{e}(i) = \mathbf{y}_m(i) + \mathbf{e}(i) \end{aligned}, \tag{2}$$

where $\mathbf{d}$ is defined in Section 2.3.

2.2.3   Case study 1

Consider the attitude of a satellite, whose attitude sensor is mounted on a flexible axial appendage. The sensor is affected by bias (0.1 mrad) and random errors (0.5 mrad, 1σ). A gyro affected by drift, bias and random error (0.1 mrad/s, 1σ) is mounted on the spacecraft.

When restricted to a single degree-of-freedom, the transfer function of the design model (see also Section 2.5) from the command torque u to the measured attitude q is fourth order as follows

$$\mathbf{P}(s) = \frac{q}{u}(s) = \frac{1}{J_0(1+\partial J)s(s\tau+1)} \frac{1}{v^2 + 2\zeta_f v + 1},$$

$$v = s/\omega_f,\ \omega_f \geq 6\ \text{rad/s},\ \zeta_f \geq 0.002,\ \tau \leq 60\ \text{s}$$

(3)

where $J_0 = 1200\ \text{kgm}^2$ is the total inertia ($\partial J = \pm 0.2$), ω_f and ζ_f are the smallest angular frequency and damping coefficient, respectively, of the flexible link between the spacecraft and the star tracker, τ is the mechanical time constant, i.e. the ratio between inertia and friction coefficient. The gyro measure $y_g(i)$ is sampled at $1/T = 100\ \text{Hz}$. The attitude measurement $y_q(i_k)$ is sampled at $1/T_q$, $T_q = N_q T$, where $N_q = 10$, and $i_k = kN_q$. The attitude q describes the inertial rotation around the spacecraft axis which must track a variable reference $\underline{q}$. The angular rate, in angular units, measured by the gyro, is denoted by ω. The command acceleration (dispatched to the reaction wheels) is $a_u = T^2 u / J$ and is bounded by $|a_u / T^2| \leq 25\ \text{mrad/s}^2$, and by $|\dot{a}_u T^2| \leq 0.250\ \text{rad/s}^3$ (slew rate).
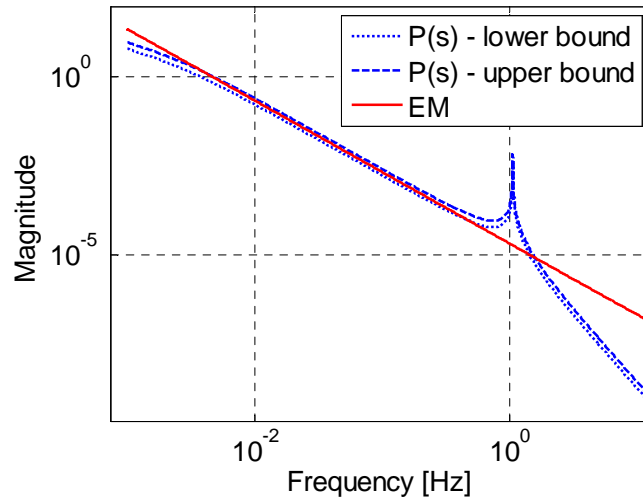

Figure 1 Case study 1: magnitude of the Bode diagrams of the design and embedded models. The embedded model $\mathbf{M}$ only accounts for rigid motion, thus confining flexible dynamics into the model error. Disturbance accelerations (drag, gravity gradient, ...) are described in Section 2.3.3 by d_a. State and multi-rate output equations are written as

$$\mathbf{x}_c = \begin{bmatrix} q_d \\ \omega_d \end{bmatrix}, \ A_c = \begin{bmatrix} 1 & 1 \\ 0 & 1 \end{bmatrix}, \ B_c = \begin{bmatrix} 1/2 \\ 1 \end{bmatrix}$$

$$y_g(i) = \omega_d(i) + e_g(i)$$

$$y_q(i_k) = q_d(i_k) + e_q(i_k)$$

(4)

where q_d and ω_d are 'dirty' variables which include systematic errors as in [7]. The dirty rate is corrected by a disturbance d_g in order to recover the 'true' rate driving q_d. Figure 1 shows the Bode plots of the uncertain design model (3) (upper and lower bounds) and of the embedded model (4). Equation (4) is observable and controllable. The reference attitude satisfies the same dynamics as in (2) and (4), but being free of the disturbance signals, is written as

$$\mathbf{x}(i+1) = A_c \mathbf{x}(i) + B_c \underline{u}(i), \ \mathbf{x}(0) = \mathbf{x}_0$$

$$\underline{y}(i) = C_c \mathbf{x}(i), \ \mathbf{x}^T = \begin{bmatrix} q & \omega \end{bmatrix}$$

(5)

where $\underline{u}$ is the open-loop (or reference) command.

2.2.4 Case study 2

Consider a ball and beam device where a dc motor rotates a beam carrying a sliding ball through a gear. The supply voltage is denoted by u, $|u| \le 6 \, \text{V}$, and is digitized as a 14-bit integer. The angle of the output gear is denoted by q, $|q| < 1 \, \text{rad}$, and is measured by an incremental encoder. The beam tilt θ is rather proportional to q since $\theta \cong \lambda q (1 - q^2/6)$ and $q^2/6 < 0.1$. The ratio $\lambda < 1$ is the arm ratio of the gear-to-beam kinematic link. Neglecting gear backlash and just considering tooth deformation, the transfer function of the design model from voltage to the gear angle is found to be

$$\mathbf{P}(s) = \frac{q}{u}(s) = \frac{b_a s^2}{s^3 (s + 1/\tau) + \Omega^4} \frac{1}{v^2 + 2\zeta_f v + 1}$$

$$v = s/\omega_f, \ \omega_f \ge 800 \, \text{rad/s}, \ \zeta_f \ge 0.0015, \ \tau \le 30 \, \text{ms}$$

(6)

The pair of zeros in the origin appearing in (6) indicate that the gear angle q (and the beam tilt) is proportional to the ball acceleration $\ddot{s}$ through $\ddot{s} \cong aq = \mu g \lambda q$, $a \cong 0.42 \, \text{m/s}^2$, where $\mu = 5/7$ is the ball equivalent mass ratio, and g is the gravity acceleration. The command gain b_a from voltage to the gear angular acceleration holds $b_a \cong 190 \, \text{V/rad/s}^2$, which value

is accurately known. The time constant $\tau = JR / \phi^2$ is the dc motor electro-mechanical constant, that depends on the assembly inertia J, on the motor resistance R and on the linked flux ϕ. The value of τ is accurately known. The fourth power of the angular frequency Ω is the product of a (gravity acceleration) and of the angular acceleration per unit length $\varpi = 10 \div 15 \text{ rad/s}^2/\text{m}$; namely $\Omega^4 = a\varpi$. The parameter ϖ accounts for the beam gravity torque and varies with the beam angle θ. Other discrepancies (friction, …) and nonlinearities (friction, backlash, …) are treated both as known and unknown disturbances. The backlash half-width d which is reckoned on the output gear holds $d \cong 1.5 \text{ mrad}$, the value being equal to the encoder quantization $\rho_q \cong 1.5 \text{ mrad}$. A dc tachometer is available, but unlike the case study 1, only the encoder output y_q in (4) is employed. The same EM as in (4), except for y_g, is employed for control design and implementation. The subscript d is dropped from the state variables in (4), since no systematic errors must be compensated. Vector and matrices of the EM state equations (2) are the following:

$$\mathbf{x}_c = \begin{bmatrix} q \\ \omega \end{bmatrix}, \ A_c = \begin{bmatrix} 1 & 1 \\ 0 & 1 \end{bmatrix}, \ B_c = \beta_a \begin{bmatrix} 1/2 \\ 1 \end{bmatrix}, \ \beta_a = b_a T^2$$

$$y_q(i) = q(i) + e_q(i) \tag{7}$$

The control time units is $T = 0.5 \text{ ms}$. The angular rate ω in (7) is an angular increment in radian units. The same reference dynamics as in (5) applies. Figure 2 shows the magnitude of the Bode diagrams of equations (6) and (7). The low frequency deviation is due to friction and to the ball-dynamics interaction through the gravity torque coefficient ϖ.
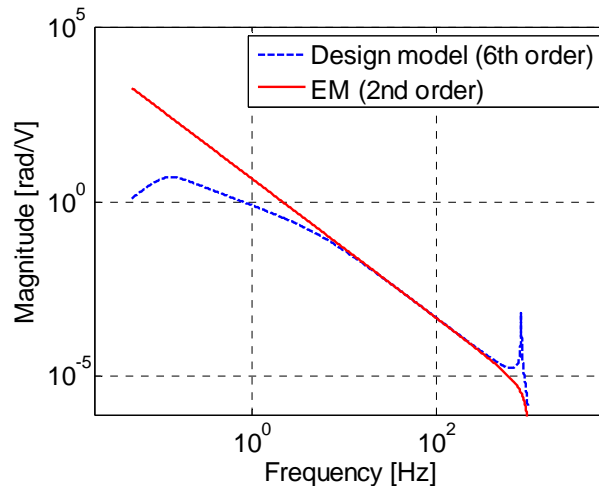
Figure 2   Case study 2: magnitude of the Bode diagrams of design and embedded models.

2.3   The uncertainty propositions

2.3.1   Propositions

Feedback regulation implicitly decreases the output sensitivity to discrepancies. Sensitivity may be further abated by explicitly rejecting disturbances as in [11], [12], [13], which calls for an explicit model of the disturbance signals. A pair of provable propositions paves the way to disturbance modeling.

1) *Proposition 3.* Model error $\mathbf{e}$, as it encodes the current outcome of past discrepancies, is the sole available measurement of the uncertain discrepancies ('uncertainty').

2) *Proposition 4.* Model error can be elaborated and accumulated in a state vector $\mathbf{x}_d$ (disturbance state), ready to correct $\mathbf{x}_c$. Formally, observable input-output dynamics $\mathbf{D}$ as in [11], [12], [13] must be built, from an input $\mathbf{w}$ to an output $\mathbf{d}$, the latter forcing $\mathbf{M}$ in parallel to $\mathbf{u}$. As a result, $\mathbf{x}_d$ encodes the past accumulated discrepancies, whereas $\mathbf{w}$ encodes the past and future independent uncertainty (innovation) capable of updating $\mathbf{x}_d$. Independence of future derives from causality, whereas independence of past answers the principle of not delaying disturbance updating. For such reasons $\mathbf{w}$, called 'noise', can be modeled as an arbitrary and bounded zero-mean signal, and statistically as a bounded-variance DT white noise.

Disturbance dynamics is widely treated in the literature [11], [12], [13], [14]; the opposite can be said of noise design [2], [6]. As a conclusion, the embedded model is forced by two input vectors: $\mathbf{u}(i)$ is known since it is computed at any i by the control unit, $\mathbf{w}(i)$ is unknown and unpredictable. How to retrieve $\mathbf{w}$ at any i is the subject of Section 2.4.

2.3.2   State equations

Assuming linearity, the disturbance dynamics is written as

$$
\begin{aligned}
\mathbf{x}_d(i+1) &= A_d\mathbf{x}_d(i) + G_d\mathbf{w}(i), \quad \mathbf{x}_d(0) = \mathbf{x}_{d0} \\
\mathbf{d}(i) &= H_d\mathbf{x}_d(i) + G_c\mathbf{w}(i) + \mathbf{h}(\mathbf{x}_c)
\end{aligned},
\tag{8}
$$

where $\mathbf{h}$ is referred to as cross-coupling term, and is discussed in Section 2.5. The state $\mathbf{x}_d$ must be observable from the output $\mathbf{y}$. The free response of (8) is used to model 'deterministic' components as in the Internal Model Control [15], assuming that $\mathbf{x}_{d0}$ is known. Usually (A_d, G_d) is controllable. On the contrary, $\mathbf{x}_d$ splits into controllable and non controllable entries. Because the latter ones only account for deterministic components, they do not need to be observable. When $H_d = B_c M_d$, $G_c = B_c N_c$ and $\mathbf{h} = B_c \mathbf{m}$, $\mathbf{d}$ is called collocated since adds to the command, which case calls for a new definition of $\mathbf{d}$ as follows

$$\begin{aligned}\mathbf{d}(i) &= \mathbf{d}_u(i) + \mathbf{w}_u(i) = \mathbf{d}_w(i) + \mathbf{m}(\mathbf{x}_c) \\ \mathbf{w}_u(i) &= M_c \mathbf{w}(i), \ \mathbf{d}_u(i) = M_d \mathbf{x}_d(i) + \mathbf{m}(\mathbf{x}_c)\end{aligned}, \tag{9}$$

where $\dim \mathbf{d}_u = \dim \mathbf{u}$.

Assumption 1. The noise $\mathbf{w}_u$ in (9) is assumed to have statistically independent entries, and to be independent of $G_d \mathbf{w}$ in (8).

2.3.3   Case study 1

The disturbance vector $\mathbf{d}$ in (8) splits into two components: the acceleration disturbance $d_u = a + w_u$, and the velocity disturbance $d_g = a/2 + s_g$, where s_g compensates the gyro systematic errors of ω_d. Second-order dynamics describes d_u, whereas first-order dynamics applies to d_g, as follows

$$\begin{aligned}
\mathbf{x}_d &= \begin{bmatrix} s_g \\ a \\ s \end{bmatrix}, \ A_d = \begin{bmatrix} 1 & 0 & 0 \\ 0 & 1 & 1 \\ 0 & 0 & 1 \end{bmatrix}, \ G_d = \begin{bmatrix} 1 & 0 & 0 & 0 \\ 0 & 0 & 1 & 0 \\ 0 & 0 & 0 & 1 \end{bmatrix} \\
\mathbf{w} &= \begin{bmatrix} w_g \\ w_u \\ w_a \\ w_s \end{bmatrix}, \ G_c = \begin{bmatrix} 0 & 0 & 0 & 0 \\ 0 & 1 & 0 & 0 \end{bmatrix}, \ H_d = \begin{bmatrix} 1 & 1/2 & 0 \\ 0 & 1 & 0 \end{bmatrix}
\end{aligned} \tag{10}$$

Noise entries are statistically independent. Equations (4) and (10) are observable, $\mathbf{d}$ is not collocated owing to d_g.

2.3.4 Case study 2

Since the dc motor velocity is not measured, only the acceleration disturbance $d_u = a + w_u$ must be modeled, which is done through a second-order stochastic dynamics as follows

$$\mathbf{x}_d = \begin{bmatrix} a \\ s \end{bmatrix}, \ A_d = \begin{bmatrix} 1 & 1 \\ 0 & 1 \end{bmatrix}, \ G_d = \begin{bmatrix} 0 & 1 & 0 \\ 0 & 0 & 1 \end{bmatrix}$$

$$\mathbf{w} = \begin{bmatrix} w_u \\ w_a \\ w_s \end{bmatrix}, \ G_c = \begin{bmatrix} 0 & 0 & 0 \\ 1 & 0 & 0 \end{bmatrix}, \ H_d = \begin{bmatrix} 1/2 & 0 \\ 1 & 0 \end{bmatrix}. \tag{11}$$

As a consequence, $\mathbf{d} = d_u$ in (8) is collocated.

2.4 The central propositions: noise estimation

2.4.1 Propositions

Propositions repeat Kalman filter results, but from a generic standpoint.

1) *Proposition 5.* Two alternative mechanisms may generate noise: pseudo-random extraction, and 'estimation' from a correlated realization. The former would respect noise statistical properties; the latter, to be adopted, reveals the residual discrepancies that are hidden in the model error, to the benefit of the embedded model as it may actually be driven by noise in order to approach the plant behaviour. Complexity and uncertainty of discrepancies usually cause the statistical framework to be abandoned in favor of a complete, but bounded, arbitrariness, which entails command independence. The latter assumption, that can be referred to as the 'Kalman assumption' in Section 2.5, does not hold in general as explained in the same Section, but justifies the noise estimation algorithm.

2) *Proposition 6.* Under the Kalman assumption, and the equations (2) and (8), the 'noise estimator (see [2] and [6]) is a linear dynamic system as follows

$$\begin{aligned} \mathbf{w}(i) &= L\mathbf{e}(i) + N\mathbf{q}(i) \\ \mathbf{q}(i+1) &= A_q \mathbf{q}(i) + B_q C_c \mathbf{e}(i), \ \mathbf{q}(0) = \mathbf{q}_0 \end{aligned}, \tag{12}$$

where the matrices L, N, A_q and B_q must be designed to make the closed-loop system (2), (8) and (12) asymptotically stable and possibly minimum variance. The closed-loop system becomes a one-step state predictor, as it provides, at any time i, predictions $\mathbf{x}_c(i+1)$ and $\mathbf{x}_d(i+1)$. To mark that states and predictions, when updated by noise realization, become, in their turn, realizations of the embedded model signals, the 'hat' notation as in $\hat{\mathbf{x}}_c(i)$ is applied to the state variables and to the model output in (2), (8) and (12), in analogy with prediction theory [16]. Indeed, $\hat{\mathbf{x}}_c(i)$ is a one-step prediction based on the past sequence $\{\mathbf{y}(i-k), k>0\}$ of the plant output. Noise estimation and model error is assigned a 'bar' notation as in $\bar{\mathbf{w}}(i)$ to mark dependence on the current output $\mathbf{y}(i)$.

A corollary that the authors never met in the literature, and is a cornerstone of EMC architecture and design is the following.

Corollary 1. The estimated noise $\bar{\mathbf{w}}$ is the sole and unique feedback channel from plant to embedded model, thus becoming responsible for stability and performance.

Remark 1. Noise estimators in Kalman filtering are static, because noise is implicitly forced to affect all the state variables. A different approach is taken here, since noise design is an essential modeling stage as in [6]. Hence, when the noise components of the embedded model are insufficient to guarantee stability by means of a proportional feedback, a dynamic feedback must be employed.

Remark 2. Noise estimator concept facilitates multi-rate treatment as in Section 2.4.2 (see also [7]), since noise must be estimated only when the relevant model error is available.

2.4.2   Case study 1

The noise estimator of (4) and (10) must be multi-rate and dynamic (as opposed to static). To be simple, a decoupling design is adopted as in [7] exploiting the different noise variance and sampling rate of the measurements. Specifically, the noise component w_g driving s_g in (10) is estimated by the attitude error $e_q = y_q - q$, the remaining noise entries in (10) are estimated by $e_g = y_g - \omega$. Since w_g drives s_g and q, a dynamic feedback as in [2] and [6] is necessary for guaranteeing closed-loop stability. The following noise estimator results

$$\overline{w}_g\left(i_k\right) = l_q \overline{e}_q\left(i_k\right) + m_q p\left(i_k\right)$$
$$p\left(i_k + N_q\right) = \left(1 - \beta_q\right) p\left(i_k\right) + \overline{e}_q\left(i_k\right). \tag{13}$$
$$\begin{bmatrix} \overline{w}_u & \overline{w}_a & \overline{w}_s \end{bmatrix}^T \left(i\right) = L\overline{e}_g\left(i\right)$$

It is of interest to compare the upper part of (13) to a static observer feedback , namely to

$$\begin{bmatrix} \overline{w}_q \\ \overline{w}_g \end{bmatrix}\left(i_k\right) = L_q \overline{e}_q\left(i_k\right). \tag{14}$$

The feedback (14) implies that d_g in (10) must be corrected to

$$d_g\left(i\right) = a\left(i\right)/2 + s_g\left(i\right) + w_q\left(i\right), \tag{15}$$

and that the 'parasitic' noise w_q mast be added to ω_d, which is contrasting the assumed smoothness of the systematic errors affecting ω_d.

2.4.3 Case study 2

The noise estimator of (7) and (11) must be single-rate and dynamic. Since w_u in (11) drives ω and q, a dynamic feedback as in [2] and [6] is necessary to guarantee closed-loop stability. The noise estimator results into

$$\begin{bmatrix} \overline{w}_u \\ \overline{w}_a \\ \overline{w}_s \end{bmatrix} = \begin{bmatrix} l_u \\ 0 \\ 0 \end{bmatrix} \overline{e}_q\left(i\right) + \begin{bmatrix} m_u \\ m_a \\ m_s \end{bmatrix} p\left(i\right),$$
$$p\left(i+1\right) = \left(1 - \beta_q\right) p\left(i\right) + \overline{e}_q\left(i\right) \tag{16}$$

where a pair of gains have been forced to zero in order to make the size of the gains to match that of the closed-loop eigenvalues. As a remark, a static noise feedback instead of (16) would compel adding a parasitic noise component to the model velocity ω, which is contrasting rigid body assumption.

2.5   *The central issue: the uncertainty model*

Noise arbitrariness, entailing command independence, cannot capture the model error complexity. For instance, parametric uncertainty, neglected cross-coupling and dynamics are command-driven, and as such they contrast noise assumptions. The solution, well known in the literature, is to dispose of an appropriate model of the uncertainty capable of detailing the

different components: see for instance the uncertainty models built by means of the Linear Fractional Transformation [1]. A similar approach is adopted here, but an intermediate model, called 'design model', is created, which is the combination of embedded and uncertainty models. However, only the embedded model must be implemented in the control unit, setting to zero all the uncertainty parts except the disturbance dynamics and noise, and the known part of $\mathbf{m}(\cdot)$ in (9) if any. An alternative is pursued by adaptive control and estimation schemes [17], [18], where command/state dependence is accounted for multiplying noise components by the same command/state signals.

Proposition 7. Command/state dependent uncertainty is modeled in two ways: (i) the cross-coupling $\mathbf{m}(\mathbf{x}_c)$ in (9) accounts for parametric uncertainty, including nonlinear approximations, (ii) the model error $\mathbf{e}$ accounts for the neglected dynamics (unstructured uncertainty) as follows

$$\mathbf{e}(i) = \partial \mathbf{P}(\mathbf{y}_m) + \mathbf{w}_y(i). \tag{17}$$

In (17) the measurement noise $\mathbf{w}_y$ and of the (uncertain) fractional error dynamics $\partial \mathbf{P}$, mapping the model output $\mathbf{y}_m$ into $\mathbf{e}$, are assumed to add. Equation (17) can be rewritten by expressing $\partial \mathbf{P}$ in terms of the design model $\mathbf{P}$ and of the embedded model $\mathbf{M}$ as follows

$$\mathbf{e}(i) = \mathbf{P}\left(\mathbf{M}^{-1}(\mathbf{y}_m)\right) - \mathbf{y}_m + \mathbf{w}_y(i), \tag{18}$$

where the former term in the RHS exists if $\dim \mathbf{y}_m = \dim \mathbf{u}$, and the response of $\mathbf{P}$ to a step $\mathbf{u}_0$ is delayed and smaller than $\mathbf{M}$, i.e.

$$\lim_{t \to \varepsilon > 0} \left|\mathbf{P}(\mathbf{u}_0)\right| / \left|\mathbf{M}(\mathbf{u}_0)\right| \le o(\varepsilon), \tag{19}$$

assuming ε arbitrarily small. In other terms, the short-term transient of the design model $\mathbf{P}$ (emulating the plant) is of higher order than the embedded model $\mathbf{M}$. If $\mathbf{P}$ and $\mathbf{M}$ are rational transfer functions, (19) converts into

$$\lim_{f \to \infty} \left|\mathbf{M}^{-1}(f)\mathbf{P}(f) - I\right| \to 1. \tag{20}$$

Zero fractional dynamics $\partial \mathbf{P} \equiv 0$ and zero cross-coupling $\mathbf{m} = 0$, can be referred to as 'the Kalman assumption', since they are necessary for Kalman filter to be unbiased and efficient.

2.5.1 Case studies

The embedded model (4), written in Laplace transform as

$$\mathbf{M}(s) = 1/\left(J_0 s^2\right), \tag{21}$$

and the fractional error dynamics

$$\partial \mathbf{P}(s) \cong \frac{\partial J - \left(v^2 + 2\zeta v\right)}{v^2 + 2\zeta v + 1} \tag{22}$$

satisfy (20). The parametric uncertainty ∂J enters (22) as a low-frequency contribution. The expression of $\partial \mathbf{P}(s)$ coming out from (6) and (7) is more complicated. The magnitude of the relevant Bode diagram is shown in Figure 3. The frequency domain splits into three regions: the low-frequency region (related to parametric errors and uncertainty) where $\left|\partial \mathbf{P}(jf)\right| \to 1$, the mid-frequency region where $\left|\partial \mathbf{P}(jf)\right| < 1$, and the high-frequency region (mainly dictated by neglected dynamics) where $\left|\partial \mathbf{P}(jf)\right| > 1$.
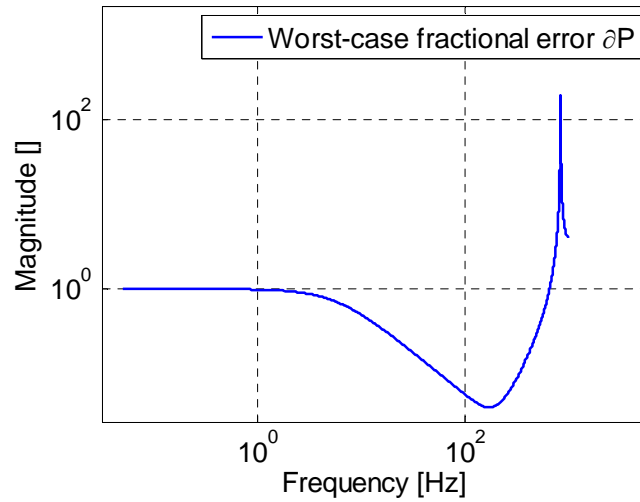
Figure 3 Case study 2: magnitude of the Bode diagram of $\partial \mathbf{P}(s)$.

3 Control propositions

Embedded and design models, as well as noise estimators are ingredients to control architecture and design. The latter splits into two stages: (i) the model-based design aims to

synthesize a control law which provides the command $\mathbf{u}$ as output, and is fed by real-time data coming from embedded model and reference signals, (ii) the uncertainty-based design (also plant-based) is in charge of tuning the gains of the estimator noise for guaranteeing stability in the presence of uncertainty. Preliminary is the definition of the control performance errors.

3.1 Performance propositions

Proposition 8. Performance is expressed by the 'true' tracking error

$$\underline{\mathbf{e}}(i) = \underline{\mathbf{x}}(i) - \mathbf{x}_c(i), \ \underline{\mathbf{e}}_y(i) = \underline{\mathbf{y}}(i) - \mathbf{y}_m(i) = C_c \underline{\mathbf{e}}(i) \tag{23}$$

where $\underline{\mathbf{x}}$ and $\underline{\mathbf{y}}$ denote the reference state and the output variables that satisfy a reference dynamics equal to the controllable dynamics (2), but disturbance-free as in (5). More generic reference dynamics can be defined by adding a known input $\mathbf{d}_0$ (not pursued here). The tracking error $\underline{\mathbf{e}}$ is only available either mathematically or through simulation, since only the predicted state and output $\hat{\mathbf{x}}_c$ and $\hat{\mathbf{y}}_m$ are available in the control unit, as the following proposition states.

Proposition 9. The only measurable errors are (i) the 'estimated' tracking error

$$\underline{\hat{\mathbf{e}}}(i) = \underline{\mathbf{x}}(i) - \hat{\mathbf{x}}_c(i) = \underline{\mathbf{e}}(i) + \hat{\mathbf{e}}_c(i), \ \underline{\hat{\mathbf{e}}}_y(i) = C_c \underline{\hat{\mathbf{e}}}(i), \tag{24}$$

which is the sum of the true tracking error $\underline{\mathbf{e}}$ and of the prediction error $\hat{\mathbf{e}}_c = \mathbf{x}_c - \hat{\mathbf{x}}_c$, and (ii) the 'estimated' model error

$$\overline{\mathbf{e}}(i) = \mathbf{y}(i) - \hat{\mathbf{y}}_m(i) = C_c \hat{\mathbf{e}}_c(i) + \mathbf{e}(i). \tag{25}$$

The following corollary links the errors in (24) and (25) to the standard control error defined as reference signal minus measurement.

Corollary 2. The control error (jitter) $\mathbf{e}_y = \underline{\mathbf{y}} - \mathbf{y}$ is the sum of the measurable tracking and model errors as follows

$$\mathbf{e}_y(i) = \underline{\mathbf{y}}(i) - \mathbf{y}(i) = \underline{\hat{\mathbf{e}}}_y(i) - \overline{\mathbf{e}}(i). \tag{26}$$

Model- and uncertainty-based design emerges from (26). (i) Model-based design aims to make negligible the 'estimated' output tracking error $\underline{\hat{\mathbf{e}}}_y(i)$, which is feasible since reference

18

and predicted state vectors in (24) are model variables. (ii) Uncertainty-based design aims to make $\bar{\mathbf{e}}(i)$ bounded in the presence of uncertainty and discrepancies. If both aims are achieved, (26) simplifies to $\mathbf{e}_y(i) \cong -\bar{\mathbf{e}}(i)$, i.e. the jitter $\mathbf{e}_y$ becomes equal to the opposite of the model error. The actual performances must be expressed through some error norm. The estimated model error written in the form

$$\bar{\mathbf{e}}(t/t) = \mathbf{y}(t) - \hat{\mathbf{y}}_m(t/t-\tau),\tag{27}$$

is employed by prediction and identification theory [16] under the name of prediction error, a name here reserved to (24), which is fully model-based. The model error

$$e = y(i) - y_m(i),\tag{28}$$

is employed as a tracking (or output) error in the Model Reference Adaptive Control [17], where the model act as a reference to be tracked by the output. A similar approach and nomenclature (reference error) is adopted by Internal Model Principle [15], and by the Model Predictive Control scheme [19], where the model role is played by the reference signal. EMC fully distinguishes between model and control errors as clarified by Corollary 2.

3.1.1   Case study 1

Target and simulated performance of the case study 1, namely the peak absolute value (max), the root mean square (RMS) and the mean value, are reported in Table 1. Simulated results refer to Figure 4, Figure 5, Figure 6 and Figure 9.

Table 2. Case study 1 -Target and simulated performance.					
No	Tracking error	Target		Simulated		
		Max	RMS	Max	RMS	Mean
0	Attitude [mrad]	0.6	0.2	0.5	0.15	0.12
1	Rate [mrad/s]	0.25	0.18	0.07	0.06	<0.002

3.1.2 Case study 2

The objective is to move the gear angle q (hence the beam tilt θ) from minimum to maximum stroke, $|q| \leq q_{max} < 0.8 \text{ rad}$, in less than $\tau_q = 0.5 \text{ s}$, while keeping the 'control error' less than the encoder quantization. Target and simulated performances as in Table 2 are

employed in Table 3. Simulated and experimental results refer to Figure 7, Figure 15, Figure 16 and Figure 17.

No	Control error	Target		Simulated (experimental)		
		Max	RMS	Max	RMS	Mean
0	Gear angle [mrad]	3	1.5	3 (1.5)	1.2 (1.2)	0.0 (0.2)

Table 3. Case study 2 -Target and simulated (experimental) performance.

3.2   Model-based control theorem

3.2.1   Fundamental theorem

When and how the tracking errors $\hat{\underline{\mathbf{e}}}$ and $\hat{\underline{\mathbf{e}}}_y = C_c\hat{\underline{\mathbf{e}}}$ can be made negligible is expressed by the following theorem.

Theorem 1. The mean 'estimated' tracking error $\hat{\underline{\mathbf{e}}}$ can be brought asymptotically to zero; the error norm $|\hat{\mathbf{e}}|$ can only be bounded because of causality.

The proof follows by considering the error equation

$$\begin{aligned}\hat{\underline{\mathbf{e}}}(i+1) &= (A_c - B_cK)\hat{\underline{\mathbf{e}}}(i) - B_c\bar{\mathbf{w}}_u(i) \\ \bar{\mathbf{w}}_u(i) &= N_w\mathbf{q}(i) + L_w\bar{\mathbf{e}}(i) \\ \mathbf{q}(i+1) &= A_q\mathbf{q}(i) + B_qC_c\bar{\mathbf{e}}(i)\end{aligned} \qquad . \qquad (29)$$

The theorem holds if and only if $A_c - B_cK$ is asymptotically stable, and $\bar{\mathbf{w}}_u$ is zero-mean and bounded. To prove (29), first write the control law in the case of a collocated disturbance, namely

$$\mathbf{u}(i) = \underline{\mathbf{u}}(i) + K\hat{\underline{\mathbf{e}}}(i) - \hat{\mathbf{d}}_u(i), \ \hat{\mathbf{d}}_u = M_d\hat{\mathbf{x}}_d + \underline{\mathbf{m}}(\hat{\mathbf{x}}_c), \qquad (30)$$

where $\underline{\mathbf{m}}$ is the known model of $\mathbf{m}$ in (9), and the estimated noise $\bar{\mathbf{w}}_u(i)$ cannot enter (30) since it occurs simultaneously with $\mathbf{u}(i)$ (causality constraint). In other terms, all the components of (30) must be one-step predictions, but noise prediction is zero. The feedback gain matrix K must be designed to make $A_c - B_cK$ asymptotically stable, which is feasible since (A_c, B_c) is controllable. Then write the tracking error equation by combining (30) with (2) and (5), which yields

$$\underline{\mathbf{e}}(i+1) = A_c\underline{\mathbf{e}} - B_cK\hat{\underline{\mathbf{e}}} - B_c(\hat{\mathbf{d}}_u - \mathbf{d}_u - \mathbf{w}_u), \qquad (31)$$

and the prediction error equation

$$\hat{\mathbf{e}}_c(i+1) = A_c \hat{\mathbf{e}}_c + B_c \left(\hat{\mathbf{d}}_u - \mathbf{d}_u + \bar{\mathbf{w}}_u - \mathbf{w}_u \right). \tag{32}$$

Summing (31) and (32), and remembering (12) provides (29). Finally, the properties of $\bar{\mathbf{w}}_u$ are guaranteed by the prediction error equation (32) being asymptotically stable, and by $\mathbf{e}$ and by the cross-coupling error

$$\Delta \mathbf{m}(\cdot) = \mathbf{m}(\mathbf{x}_c) - \underline{\mathbf{m}}(\hat{\mathbf{x}}_c) \tag{33}$$

being bounded. The latter condition is immediately satisfied under the Kalman assumption, since $\mathbf{e} = \mathbf{w}_y$, and $\Delta \mathbf{m} = 0$.

Remark. In general, $\Delta \mathbf{m}(\cdot)$, which depends on $\hat{\mathbf{e}}_c(i)$ through $\mathbf{x}_c$ and $\hat{\mathbf{x}}_c$, cannot be bounded unless (30) is suitably designed versus $\Delta \mathbf{m}(\cdot)$, which calls for robust control design [1]. On the other hand, since $\Delta \mathbf{m}(\cdot)$ is unknown except for some bound, it can be treated as an unknown component of the total disturbance $\mathbf{d}_u$, and as such, it can be estimated by $\hat{\mathbf{x}}_d$. As a consequence, $\Delta \mathbf{m}(\cdot)$ must be bounded by the state predictor design (Section 3.3), whose task is that of estimating $\hat{\mathbf{x}}_d$.

The following corollary states that (29) cannot be improved.

Corollary 3. Noise rejection can only enter (30) if delayed, i.e. through $\bar{\mathbf{w}}_u(i-k)$, $k > 0$, which implies that the difference $\bar{\mathbf{w}}_u(i) - \bar{\mathbf{w}}_u(i-k) \neq 0$ may replace $\bar{\mathbf{w}}_u(i)$ in (29), but the difference has a norm larger than $\bar{\mathbf{w}}_u(i)$ in the case of a statistically independent noise.

The ideal, unrealizable case

$$\underline{\hat{\mathbf{e}}}(i+1) = (A_c - B_c K) \underline{\hat{\mathbf{e}}}(i) \Rightarrow \lim_{i \to 0} \underline{\hat{\mathbf{e}}}(i) = 0 \tag{34}$$

is referred to as the 'anti-causal' limit. The asymptote (34) is approached as soon as the eigenvalues of $A_c - B_c K$ becomes faster (closer to zero). Such a design guideline agrees with the model-based control law (30), but departs from standard robust design in [1], [20] and [21], where feedback gains are responsible for plant-based stability and performance. In the anti-causal limit, prediction and tracking errors may substitute each other asymptotically, which is assumed hereafter, since

$$\lim_{i \to \infty} \left(\underline{\mathbf{e}}(i) + \hat{\mathbf{e}}_c(i) \right) = 0. \tag{35}$$

.*Proposition 10.* The gain K in (30) must be designed to push the eigenvalues of $A_c - B_c K$ toward zero (deadbeat control) so as to minimize the effect of the not rejected noise components on the tracking error. The only limit comes from a bounded control authority (range and slew rate), as in the linear quadratic optimal control. In this sense, the feedback control design only depends on the causal uncertainty expressed by the noise, and not on parametric and unstructured uncertainties (model-based design).

Remark. Severe limitations of the control authority make the 'anti-causal limit' assumption invalid, and call for a non-standard design which departs from Proposition 10. In that case, the design of K may de driven by uncertainty.

3.2.2 Case study 1

The control law following (30) becomes

$$a_u(i) = \underline{a}_u + k_q \left(\underline{q} - \hat{q}_d \right) + k_\omega \left(\underline{\omega} - \hat{\omega}_d - \hat{s}_g \right) - \hat{a}, \tag{36}$$

where the rate tracking error $\underline{\omega} - \hat{\omega}_d$ has been corrected by subtracting s_g for compensating gyro systematic errors.
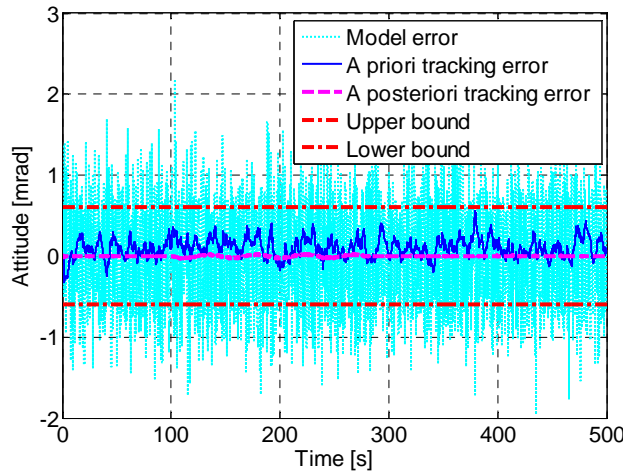
Figure 4 Case study 1 : true and estimated tracking error, and model error.

Figure 4 shows the true (solid) and estimated tracking (dashed) errors of the attitude q in (3) , that are compared to the estimated model error (dotted). The estimated tracking error is

practically zero - marking a standard design in the light of Proposition 10 -, whereas the true tracking error is the opposite of the model error (not perceivable from Figure 4), but is free of the high frequency sensor noise though is affected by bias.

Were the noise estimator implemented as a static feedback as in (14), the tracking error would become noisier owing to the 'parasitic' noise w_q in (15). Figure 5 and Figure 6 allow comparison between the dynamic design in (13) and the static one in (14). For instance, enlargement of the 'static' error in Figure 6 reveals significant oscillations of the flexible link passing through $\bar{w}_q$. A remedy would be either a narrower bandwidth (BW) or a notch filter, which latter artifice, suffering of tuning, is not in the need of the dynamic design.
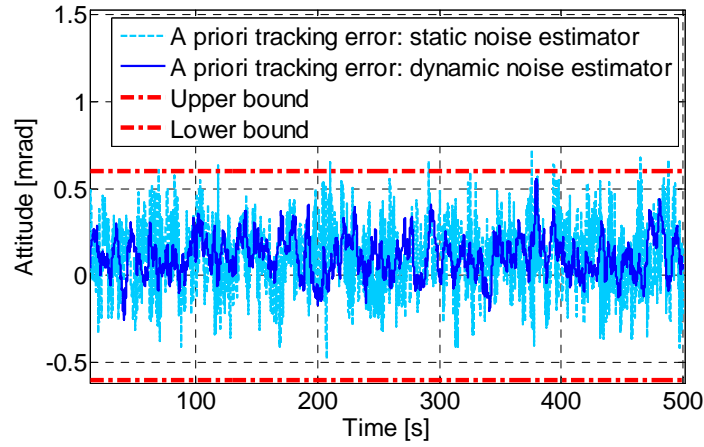
Figure 5 Case study 1: dynamic and static noise estimator.
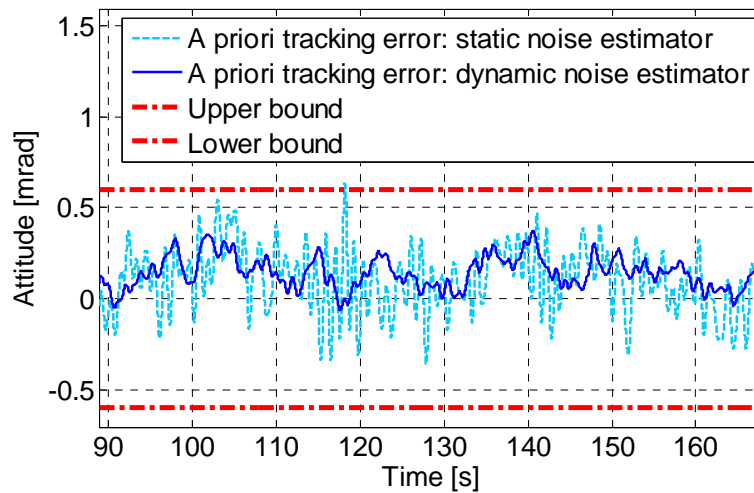
Figure 6 Case study 1: enlargement of Figure 5.

3.2.3   Case study 2

The control law has the same form as (36) except for $\hat{s}_g = 0$ and for the known disturbance term $\underline{m}$ (angular acceleration). In terms of the voltage u, the control law is found to be

$$u(i) = \underline{u} + \left(k_q \left(\underline{q} - \hat{q} \right) + k_\omega \left(\underline{\omega} - \hat{\omega}_d \right) - \hat{a} - \underline{m} \left(\hat{\mathbf{x}}_c \right) \right) / \beta_a . \qquad (37)$$

In (37) $\underline{u}$ is the reference command; the other terms, divided by β_a, are angular increments (in radian units) according to the DT model in (7). The known term $\underline{m}$ accounts for gravity torque and known friction components. Comparison between simulated tracking and control errors is done in Figure 7. 'True' tracking and control errors are affected by the combination of gear backlash and static friction (the angular position halts at about ± 1 mrad). The control error is further affected by the encoder quantization equal to 1.5 mrad. The 'estimated' tracking error is negligible, indicating that the noise estimator is effective in avoiding the backlash contribution to the model error from spilling through embedded model and control law (Section 3.3).
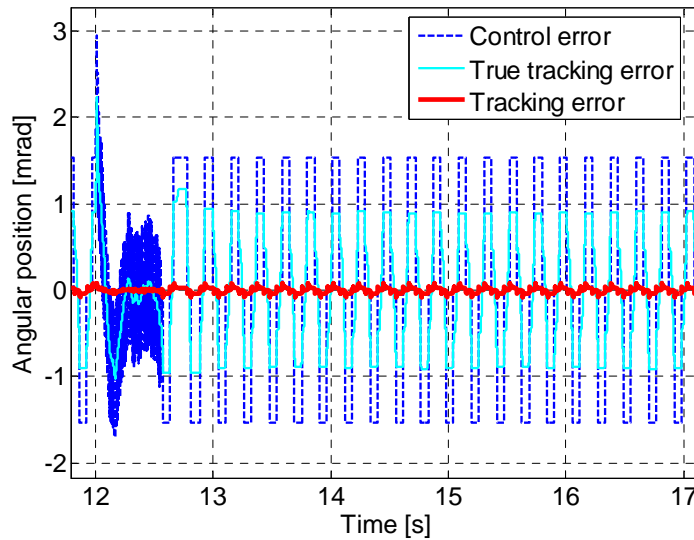

Figure 7   Case study 2: simulated tracking (true and estimated) and control error.

3.3   Uncertainty-based control design

3.3.1   Basic concepts

Abandoning the Kalman assumption opens the 'robust' control domain: the goal is still to guarantee Theorem 1, but in the presence of neglected dynamics and cross-coupling errors. Formally one has to show that $\overline{\mathbf{w}}_u$ in (29) being correlated with tracking errors, modifies the closed-loop dynamics in (29) with uncertain components. To simplify derivation yet to outline the main results, the anti-causal limit (35) is assumed, which allows to rewrite the prediction error equation (32) in terms of the true tracking error as follows

$$
\begin{aligned}
\underline{\mathbf{e}}(i+1) &= \left(A_c - B_c L_w C_c\right)\underline{\mathbf{e}}(i) + \left(A_c - B_c K\right)\hat{\underline{\mathbf{e}}}(i) - B_c\left(M_d \hat{\mathbf{x}}_d + N_w \mathbf{q}\right) + \\
&+ B_c L_w \left(\mathbf{e} - \mathbf{d}_y\right)(i), \ \underline{\mathbf{e}}(0) = \underline{\mathbf{e}}_0 \\
\underline{\mathbf{e}}_y(i) &= C_c \underline{\mathbf{e}}(i) - \mathbf{d}_y(i)
\end{aligned}
\tag{38}
$$

In (38), the state equations of $\hat{\mathbf{x}}_d$ and $\mathbf{q}$ have been omitted, and $\mathbf{d}_y$ is the output disturbance, i.e. the collocated disturbance $\mathbf{d}$ in (9) when shifted with the help of (33) to the output of the controllable dynamics. The state equation of $\mathbf{d}_y$ is

$$
\begin{aligned}
\mathbf{x}_y(i+1) &= A_c \mathbf{x}_y(i) + B_c\left(\mathbf{d}_w(i) + \Delta\mathbf{m}(\cdot)\right) \\
\mathbf{d}_y(i) &= C_c \mathbf{x}_y(i)
\end{aligned}
\tag{39}
$$

It is not difficult to recognize the predictor sensitivity $\mathbf{S}_m$ (high-pass filter) and the complement $\mathbf{V}_m = I - \mathbf{S}_m$ (low-pass filter) in (38). $\mathbf{S}_m$ and $\mathbf{V}_m$ allow rewriting the forced response of the output tracking error $\underline{\mathbf{e}}_y$ in (38) in the operator form:

$$
\begin{aligned}
\underline{\mathbf{e}}_y &= -\mathbf{S}_m \cdot \mathbf{d}_y + \left(I - \mathbf{S}_m\right)\cdot \mathbf{e} \\
\mathbf{S}_m \cdot \mathbf{d}_y &= \mathbf{d}_y(i) - \sum_{k=1}^{i} C_m A_m^{i-k} B_m \mathbf{d}_y(k-1)
\end{aligned}
\tag{40}
$$

where C_m, A_m and B_m are the state predictor matrices from (38). Equation (40) calls for the following Lemma.

Lemma 1. The effect of the neglected dynamics $\partial\mathbf{P}$ encoded in $\mathbf{e}$ on the output tracking error $\underline{\mathbf{e}}_y$ is attenuated (and bounded) by the high-pass filter $\mathbf{V}_m$, whereas the effect of the parametric uncertainty $\Delta\mathbf{m}$ encoded in $\mathbf{d}_y$ is attenuated (and bounded) by the low-pass filter $\mathbf{S}_m$. These objectives are contrasting and may become unfeasible. For this reason, artifices

like notch filters capable of cancelling the effect of the neglected dynamics on the plant measurements may be welcome. But they must be formulated as band-pass filters in the disturbance dynamics (8).

Making explicit the tracking error $\underline{\mathbf{e}}$ in $\partial \mathbf{P}(\mathbf{y}_m)$ and in $\Delta \mathbf{m}$ by means of (33), equation (40) becomes an implicit equation in $\underline{\mathbf{e}}$, which when solved, shows the uncertainty effects on the whole closed-loop system, and leads to prove 'robust' stability conditions as in the literature [20], [21]. As a departing point, EMC conditions pivot on the state predictor, hence on the embedded model and the noise estimator. The relevant development is not pursued here for brevity's sake: some results can be found in [1] and [6]. Stability conditions are shown graphically in the case study below.

Proposition 11. Under the 'anti-causal' limit (34), the main tool for reducing and bounding uncertainty effects on the tracking error, so as to guarantee plant closed-loop stability and performance (plant-based design), is the noise estimator design. According to Lemma 1 two contrasting objectives must be met, which requires a careful design of the disturbance dynamics (8), including state variables, noise and the known components of $\mathbf{m}(\cdot)$. The feedback gain K may contribute to stability only when the anti-causal limit should be abandoned, what is obliged by a limited control authority.

3.3.2   Case study 1

Figure 8 shows the Nyquist plot of the scalar transfer function $\partial \mathbf{P}(s)$ of the neglected dynamics (worst-case) in (22), before and after being passed through $\mathbf{V}_m(s)$. A sufficient stability condition under the anti-causal limit is

$$\max_{|f| \leq f_{\max}} \left| \mathbf{V}_m(jf) \partial \mathbf{P}(jf) \right| < 1, \tag{41}$$

which is not met by either design. However, the dynamic design (solid line) is largely far from encircling $(-1, 0)$ unlikely the static case (dashed line).

A more complete survey can be made by plotting the RMS of the attitude and of the angular rate tracking errors, the RMS of the command a_u in (36) and of the torque transmitted by the flexible link (in acceleration units) versus the complementary eigenvalue

$\gamma_q = 1 - \lambda_q = \left(2\pi T_q\right)^{-1} f_q$ of the noise estimators (13) and (14). The frequency f_q approaches the state predictor BW. Eigenvalues λ_q, assumed to be each other equal, uniquely fix the estimator gains. The error RMS can be estimated by Lyapunov equation.
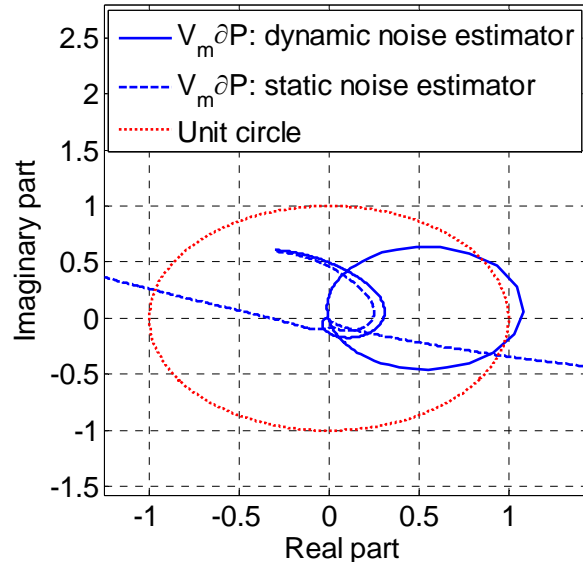

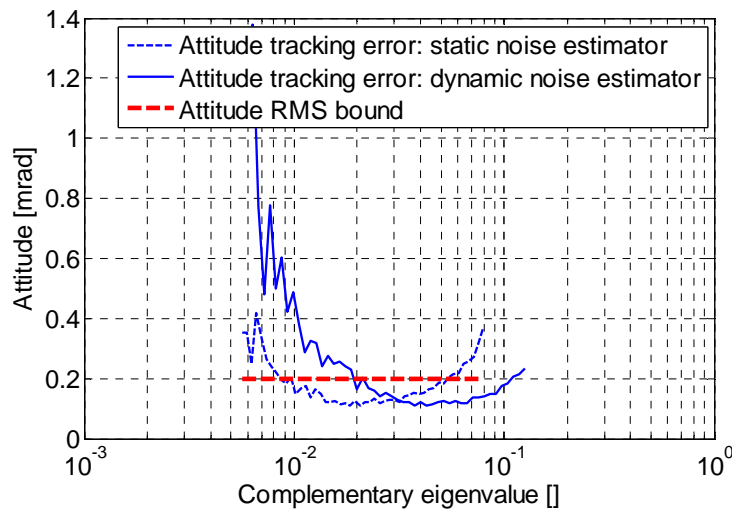Figure 8 Case study 1: Nyquist diagram of the fractional error dynamics.

Figure 9 Case study 1: attitude tracking error versus γ_q.

Figure 9 plots the tracking error RMS versus γ_q, thus indicating how much the bandwidth of the static case (dashed line) should be narrowed for repeating the dynamic case (solid line)

performance. All the simulated results below refer to $\gamma_q = 0.03$, that is to $f_q \cong 0.05\,\mathrm{Hz}$, where static (dashed line) and dynamic (solid line) performance approaches each other.
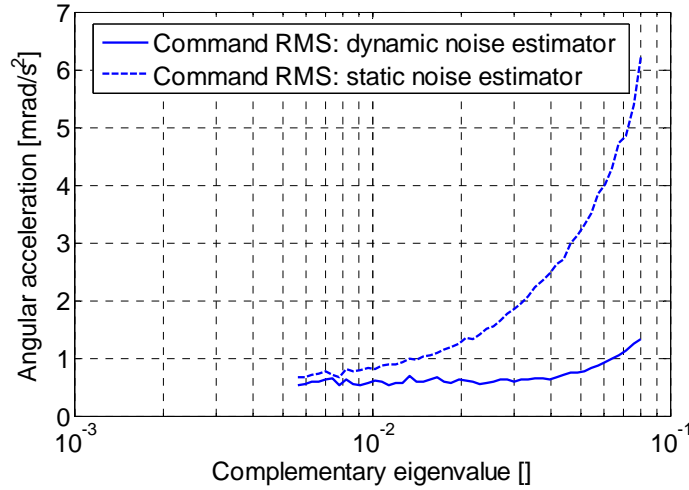

Figure 10 Case study 1: RMS of the commanded acceleration versus γ_q.

The smaller stability margin of the static case in the case of equal bandwidth, a fact that was already pointed out in Figure 8, can be better observed by comparing the command RMS (or which is the same the torque transmitted by the flexible link) in Figure 10, under zero reference, i.e. for $t \geq 300\,\mathrm{s}$ in Figure 11. Above $\gamma_q = 0.01$, the static RMS (dashed line) increases approaching instability, whereas the dynamic design (EMC, solid line) keeps the same effort over a large band, thus revealing robustness.
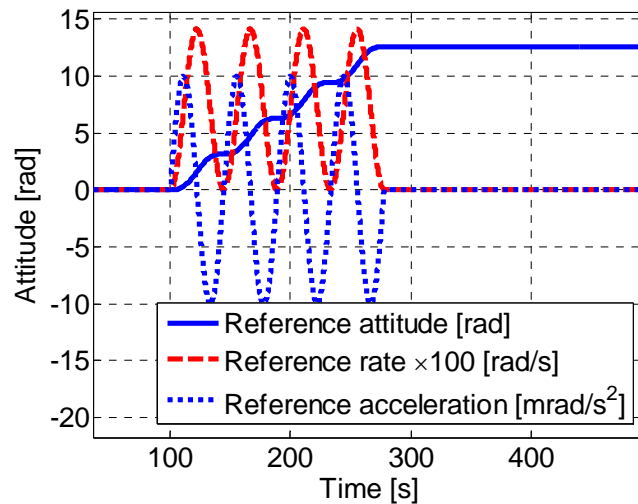
Figure 11 Case study 1: reference signals.

All the simulated results assume the reference signals in Figure 11, as they aim to progressively rotate the payload on the top of the flexible link by a succession of half-turn steps.

Figure 12 shows the commanded acceleration for the static (faint colour) and dynamic noise estimators. Static design approaches the command bound of 0.025 rad/s^2. Figure 13 compares the simulated disturbance (solid line) including drag, gravity, and other torques, with the rejected disturbance (dashed line) which is estimated by the embedded model. It is clear that the rejected disturbance is capable of implicitly estimating the parametric uncertainty ∂J of the body inertia, as it is amplified by the reference command in Figure 11 during the interval $100 \leq t \leq 300$ s. In this manner, it fully relieves the model-based control law (36) from being designed against uncertainty.
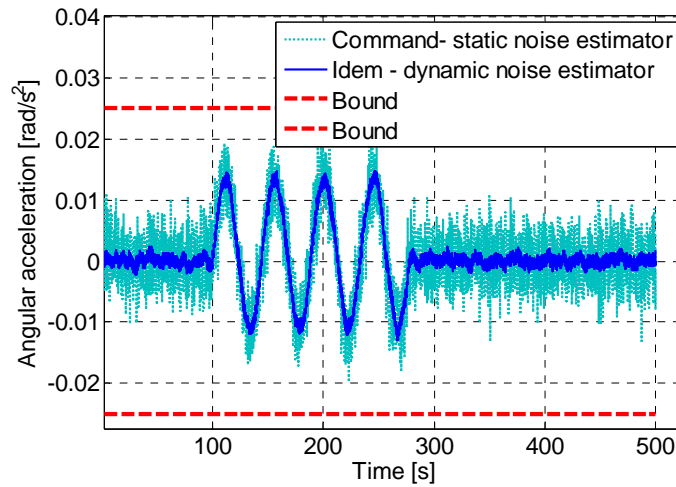

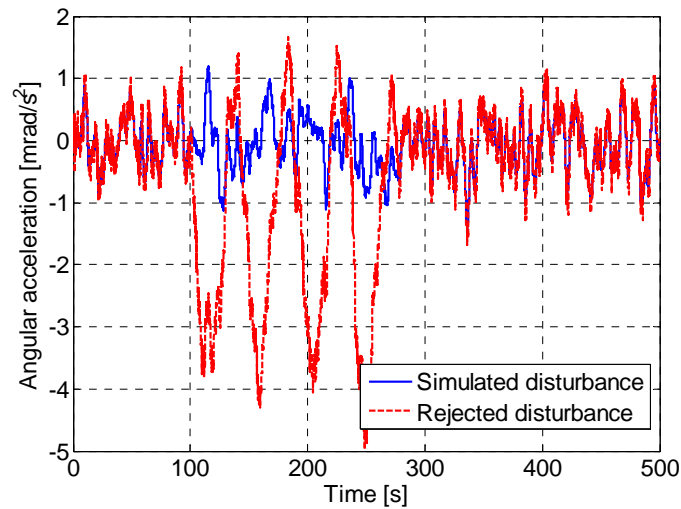Figure 12 Case study 1: commanded acceleration.

Figure 13 Case study 1: simulated and rejected disturbance.

The list of the complementary eigenvalues $\gamma_k = 1 - \lambda_k$, $k = 1,...,n$ is reported in Table 2.

No.	Control section	Size n	Value γ_k	Frequency f_k [Hz]	Nyquist f_{max} [Hz]
	Table 4. Complementary eigenvalues of the case study 1				
0	State predictor – attitude (13)	3	0.03	0.048	5
1	Idem –rate (13)	3	0.03	0.48	50
2	Feedback control (36)	2	0.1	1.6	50

As anticipated in Section 3.1.2, the feedback control eigenvalues fixing the gains k_q and k_ω in (36) are faster than the state predictor. They have been fixed somewhat below the Nyquist frequency f_{max} to guaranteeing the command effort to stay within bounds less some margin as shown in Figure 12.

3.3.3 Case study 2

The trapezoidal angular position measured by the gear encoder is shown in Figure 14. The difference between reference and measured angle- the control error – has been already plotted in Figure 7, but it can be perceived from Figure 15, when the reference angle reaches the maximum value. The measured position reaches the maximum value after a damped oscillation ending in the limit cycle (the square wave overlapping the constant reference) imposed by backlash, friction and encoder quantization. The latter cannot be rejected [22] as its magnitude is less than the encoder quantization. Figure 14 also shows the ball stroke (both

30

simulated and experimental), that, being uncontrolled, swings between the beam extremes with some delay because of friction. The bottom extreme reveals measurement irregularities due to the beam surface.
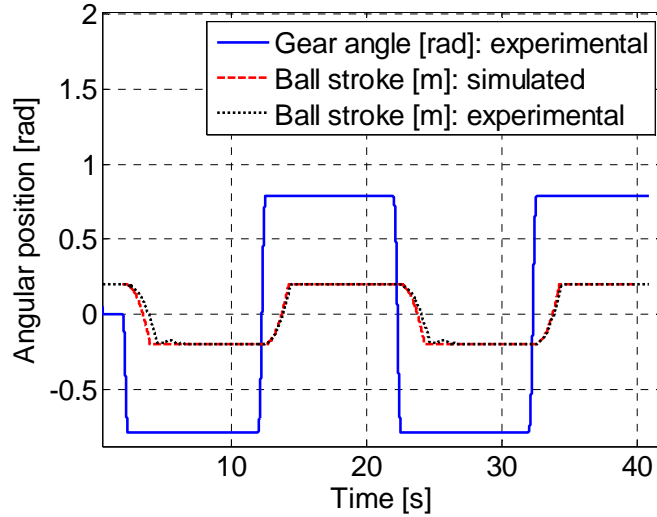

Figure 14 Case study 2: reference and actual gear angular position (measured).

The transient oscillation in Figure 15 is the same as in Figure 7, left hand side, and would disappear by adding an appropriate disturbance term $\underline{m}$ in (37). To prove this, consider Figure 16 where the measured angular position is plotted from simulated and experimental runs. The experimental measurement is free of the transient oscillation because an appropriate $\underline{m}$ has been inserted in (37) to account for viscous and static friction. The result highlights the different frequency bands where $\hat{a}$ and $\underline{m}(\hat{\mathbf{x}}_c)$ counteract the plant uncertainty. Assuming the 'anti-causal limit', $\hat{a}$ is estimated within the BW of the sensitivity $\mathbf{S}_m$ in (40). On the contrary, $\underline{m}(\hat{\mathbf{x}}_c)$, depending on the controllable state $\hat{\mathbf{x}}_c$, is estimated within the control law BW, which, in absence of command limitations, may approach the Nyquist frequency $f_{\max} = 0.5/T = 1\,\mathrm{kHz}$.
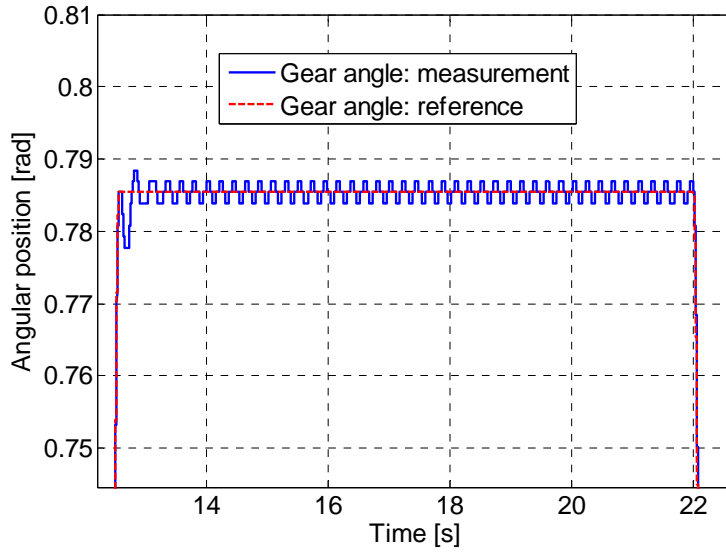
Figure 15 Case study 2: enlargement of Figure 14.

The limit cycles in Figure 16 are different in their period because of a different static friction. The experimental measurement in Figure 16, though slightly biased with respect to the simulated profile, certifies that the design model is a faithful description of the real plant.
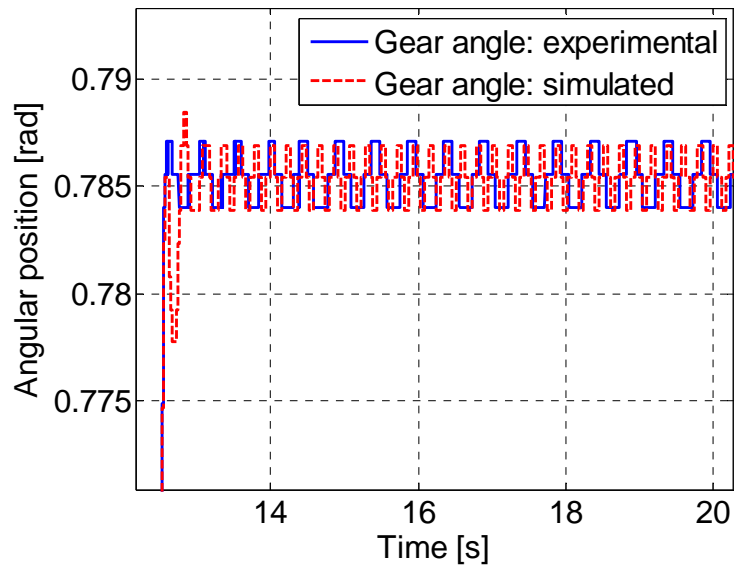

Figure 16 Case study 1: experimental and simulated measured angular position.

Figure 17 shows the total command u (solid line), the reference command $\underline{u}$ (the small square wave around 2 and 12 s, dashed line) and the estimated disturbance $\hat{a}/\beta_a$ under

$\underline{m} = 0$ (dotted line). The latter component (opposite to u) mainly accounts for friction especially during acceleration phases. Friction can be estimated from Figure 17 and explicitly accounted by $\underline{m}$.
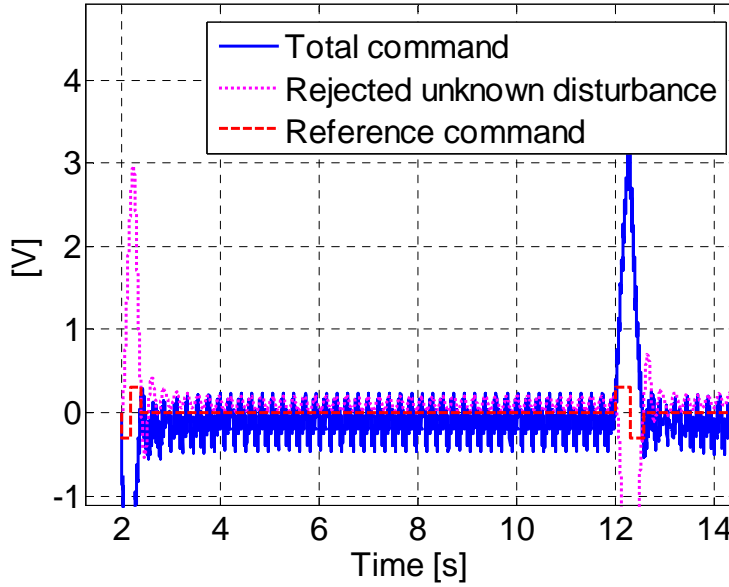

Figure 17 Case study 2: command voltage and its components.

Table 5 shows the complementary eigenvalues of the state predictor, which fix the noise estimator gains in (16), and of the control law, which fix the gains k_q and k_ω in (37). The state predictor eigenvalues have been selected to guarantee stability in the presence of neglected dynamics as in the case study 1. To this end, the resulting BW is rather narrower (less than 1/100, the same order as in Table 4) than the Nyquist frequency f_{max}. Also the control BW has been selected smaller than f_{max} for providing the command voltage u with a margin during acceleration phases.

No.	Control section	Size n	Value γ_k	Frequency f_k [Hz]	Nyquist f_{max} [Hz]
	Table 5. Complementary eigenvalues of the case study 2				
0	State predictor (16)	5	3×0.02, 2×0.03	6.4	1000
1	Feedback control (37)	2	0.2	64	1000

4 CONCLUSIONS

The key result is that the model-based control theorem fixing the control law - under the anti-causal limit - can be designed on the basis of the embedded model without reference to uncertainty. Since parametric uncertainty and unknown cross-coupling become part of the unknown disturbance signals, they can be accommodated by the noise estimator, whose task is estimating the driving noise in real-time. The estimated noise updates the state of the disturbance dynamics (to be explicitly modeled) and becomes the unique feedback channel through which plant-to-model discrepancies pass, and, if wisely filtered from the effects of the neglected dynamics, may continuously update the model state. It is essential to the results, that the control unit runs an embedded model enriched by the noise-driven disturbance dynamics, in parallel to the plant.

5 REFERENCES

[1] K. Zhou, J. C. Doyle, K. Glover, Robust and optimal control, Prentice Hall, Upper Saddle River, NJ, 1995.

[2] E. Canuto, Embedded Model Control: outline of the theory. ISA Trans., 2007, 46 (3): 363-377.

[3] M.K. Senehi, T. Kramer, A Framework for Control Architectures; International Journal of Computer Integrated Manufacturing; 1998, 11 (4): 347-363.

[4] M. H. Hamilton, W. R. Hackler, Universal Systems Language: lessons learnt from Apollo, Computer, 2008: 34-43.

[5] J. S. Albus, RCS: a reference model architecture for intelligent control, Computer, 1992: 56-59.

[6] E. Canuto, A. Molano, L. Massotti, Drag-free control of the GOCE satellite: noise and observer design, IEEE Trans. Control Systems Technology, 2010, 18 (2): 501-509.

[7] E. Canuto, A. Molano-Jimenez, C. Perez-Montenegro, Disturbance rejection in space applications: problems and solutions, Acta Astronautica, 2012, 72: 121-131.

[8] M. Keshmiri, A.F. Jahromi, A. Mohebbi, M.H. Amoozgar, W-F.Xie, Modelling and control of a ball and beam system using model based and non-model based control approaches, Int. J. on Smart Sensing and Intelligent Systems, 2012, 5 (2): 14-35.

[9] L. Zadeh, From circuit theory to system theory, Proc. of the IRE, 1962, 50 (5): 856-865

[10] R. E. Kalman, On the general theory of control systems, in Proc. Int. Congress on Automatic Control, Moscow, USSR, Academic Press, New York, 1960.

[11] K. R. Muske, T. A. Badgwell, Disturbance modelling for offset-free linear model predictive control, Journal of Process Control, 2002, 12: 617-632.

[12] C. D. Jonson, Disturbance accommodating control: an overview", Proc. American Control Conference, June 18-20, 1986, Seattle, WA, USA, 526-536,

[13] G. Tian, Z. Gao, From Poncelet's Invariance Principle to Active Disturbance Rejection, Proc. 2009 American Control Conference, St. Louis, MO, June 10-12, 2009: 2451-2457.

[14] J. B. Froisy, Model predictive Control – Building a bridge between theory and practice, Computers and Chemical Engineering, 2006, 30: 1426-1435.

[15] B. A. Francis, W. M. Wonham, The internal model principle of control theory, Automatica, 1976, 12 (5): 457-465.

[16] L. Ljung, System Identification. Theory for the user. Prentice-Hall, Englewood Cliffs, NJ, 1987.

[17] S. Sastry, M. Bodson, "Adaptive Control. Stability, convergence and robustness. Prentice-Hall, Englewood Cliffs, NJ, 1999.

[18] J-J. E. Slotine, W. Li, Applied nonlinear control. Prentice-Hall, Englewood Cliffs, NJ, 1991.

[19] E. F. Camacho, C. Bordons, Model Predictive control. Springer, New York, 2003.

[20] J. Maciejowski, Multivariable feedback design, Addison Wesley, 1989.

[21] J. C. Doyle, B. A. Francis, A. R. Tannenbaum, Feedback control theory. Macmillan, New York, 1992.

[22] C-Y. Su, Y. Stepanenko, J. Svoboda, T.P. Leung, Robust adaptive control of a class of nonlinear systems with unknown backlash-like hysteresis, IEEE Trans. Automatic Control, 2000, 45 (12), 2427-2432.